Population genetics of *Glossina palpalis gambiensis* in the sleeping sickness focus of Boffa (Guinea) before and after eight years of vector control: no effect of control despite a significant decrease of human exposure to the disease

Moise S. Kagbadouno[1], Modou Séré[2], Adeline Ségard[3,4], Abdoulaye Dansy Camara[1], Mamadou Camara[1], Bruno Bucheton[1,3,4], Jean-Mathieu Bart[1,3,4], Fabrice Courtin[3,4,5], Thierry de Meeûs[3,4$*] Sophie Ravel[3,4$]

1 Programme National de Lutte contre la THA, Ministère de la Santé, Conakry, Guinée.
2 University of Dédougou, Dédougou B.P. 176, Burkina Faso.
3 Univ Montpellier, IRD, Cirad, Intertryp, Baillarguet, 34398 Montpellier Cedex 5, France.
4 IRD, Intertryp, UMR 177, Montpellier, France.
5 Représentation de l'IRD au Burkina Faso, 668, avenue, Pr Joseph Ki-Zerbo-Koulouba, 01 BP 182 Ouagadougou 01, Burkina Faso.

Moise Kagbadouno: moise.kagbadouno@gmail.com; Modou Séré: modousere11@gmail.com; Adeline Ségard: adeline.segard@ird.fr; Abdoulaye Dansy Camara: camaradansy@gmail.com; Mamadou Camara: mamadycamarafr@yahoo.fr; Bruno Bucheton: bruno.bucheton@ird.fr; Jean-Mathieu Bart: jean-mathieu.bart@ird.fr; Fabrice Courtin: fabrice.courtin@ird.fr; Thierry de Meeûs: thierry.demeeus@ird.fr; Sophie Ravel: sophie.ravel@ird.fr

$ equal supervision

*Corresponding author: thierry.demeeus@ird.fr

Index keywords: Tsetse flies, Human African Trypanosomiasis, Population structure, Effective population size, Vector control, Neglected Tropical Diseases.

Abstract

Human African trypanosomosis (HAT), aka sleeping sickness, is still a major concern in endemic countries. Its cyclical vector are biting insects of the genus *Glossina* or tsetse flies. In Guinea, the mangrove ecosystem contains the main HAT foci of Western Africa. There, the cyclical vector is *Glossina palpalis gambiensis*. A still ongoing vector control campaign (VCC) started in 2011 in the focus of Boffa, using tiny targets, with a significant impact on the prevalence of the disease. To assess the sustainability of these results, we have studied the impact of this VCC on the population biology of *G. p. gambiensis* in Boffa. We used the genotyping at several microsatellite markers and population genetics tools of tsetse flies from different sites and at different dates before and after the beginning of the VCC. In variance with a significant impact of VCC on the apparent densities of flies captured in the traps deployed, the global population of *G. p. gambiensis* displayed no genetic signature of control, and behaved as a very large population occupying the entire zone. This implies that targets deployment efficiently protects the human populations locally, but not where targets cannot be deployed and where the main tsetse population exploits available resources. This also entails the pursuit of vector control measures until HAT can be considered as entirely eradicated from the focus.

Introduction

Human African trypanosomosis (HAT), aka sleeping sickness, is still a major concern for the WHO (Holmes, 2014; Simarro et al., 2015). Its agent is an euglenozoan kinetoplastid parasite, *Trypanosoma brucei gambiense* 1 (Jamonneau et al., 2019) (Tbg1), with a clonal propagation (Mathurin Koffi et al., 2009; M. Koffi et al., 2015), which recently emerged 10,000 years ago and spread from West Africa (W. Weir et al., 2016). It encompasses a complex life cycle, with a phase in blood sucking insects of the genus *Glossina* (Diptera, Hippoboscoidea), its cyclical vector (Bouyer et al., 2015).

In Guinea, the mangrove ecosystem still contains the main HAT foci of Western Africa (Simarro et al., 2015). There, *Glossina palpalis gambiensis* is the only known vector of the disease (Courtin et al., 2015). Boffa, is one of the three active HAT foci of the country (Kagbadouno et al., 2012). An active vector control campaign (VCC), aiming at reducing the human/tsetse contact, and subsequently at interrupting the transmission of Tbg1, was implemented in 2011 (Courtin et al., 2015).This VCC produced a significant decrease in exposure risks and prevalence of the disease (Courtin et al., 2015). As regard to the vertebrate host, the exact role of animal or asymptomatic human reservoirs is still uncertain. Nevertheless, the genetic diversity of this parasite maintained by the Guinean populations suggests the existence of a significant amount of individuals clones outside the patients involved in surveys (Mathurin Koffi et al., 2009), in human and/or animal reservoirs. Several other studies appeared to confirm this hypothesis (Bucheton et al., 2002; Büscher et al., 2018).

A recent study of *G. palpalis palpalis* in the focus of Bonon (Côte d'Ivoire), revealed that a special allele at a given trinucleotide locus (GPCAG), experienced a brutal increase in frequency after control (Berté et al., 2019). This suggested the selection for resistance against control measure.

Given these observations, deciding what strategies to use in the future will depend on the most precise knowledge we can get on the population impact of medical campaigns and VCC.

In this paper, we investigated the impact of VCC over 11 years on the HAT focus of Boffa (Figure 1). We report here the impact of VCC on capture densities and sex-ratio, as well as on *G. palpalis gambiensis* population genetics, in particular on locus GPCAG. We then discuss the best strategy to be used to optimize the protection of human populations from this neglected tropical disease.

Material and Methods

Data collection

All sites used for the entomological survey, number of trapped flies and their gender can be seen in Kagbadouno et al's paper (Kagbadouno et al., 2012) and Supplementary file S1.

Localization, date of sampling and number of genotyped flies can be found in Figure 1 and Table 1. A total of 290 flies were genotyped at 11 loci. Vector control was implemented with tiny targets from February 2012 in the sites of the left bank of river Rio Pongo and then on both sides after 2016. Then, according to Table 1, flies from 2009 and 2011 samples correspond to T0 (before control) on both sides of River Rio Pongo, while samples from 2019 and 2020 correspond to TX (after control has begun), on both sides of the river.

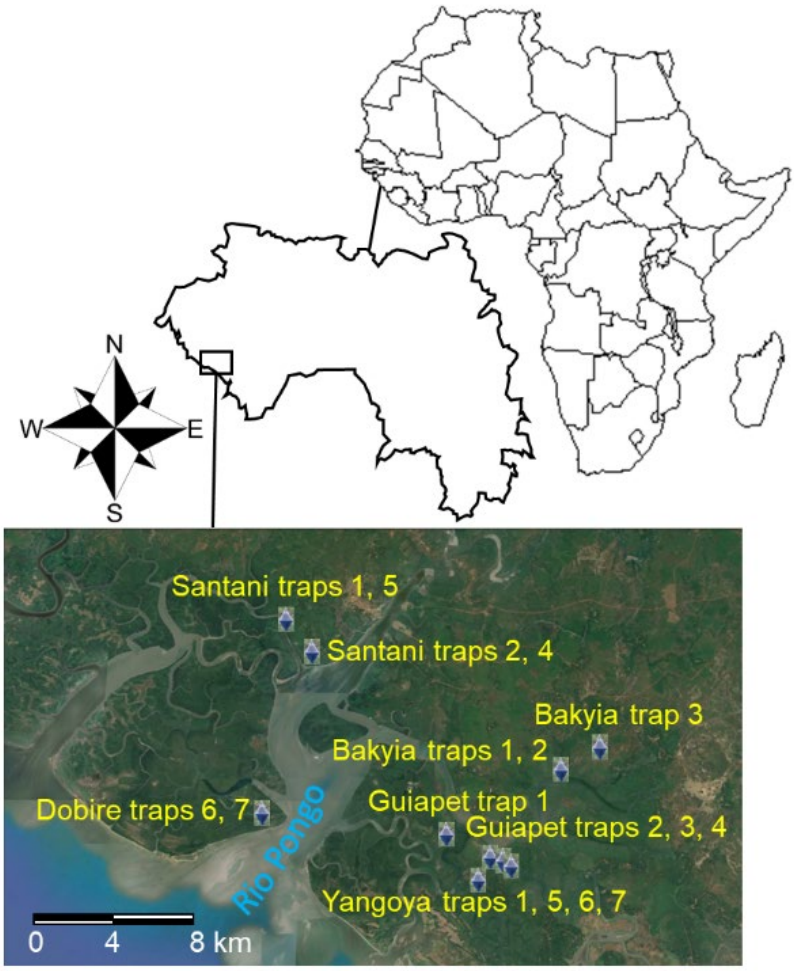

Figure 1: Localization of traps for the capture of *Glossina palpalis gambiensis* in the HAT focus of Boffa in Guinea. Dates of capture, number of flies genotyped, and other geographical information can be found in the Table 1.

Table 1: Number of genotyped *Glossina palpalis gambiensis* (*N*) in the different traps of different sites and date of capture in the HAT Focus of Boffa (Guinea). The cohort (considering six generations of tsetse flies per year) and the time (T) after the beginning of control in months (0=before), the bank of the Rio Pongo River (see Figure 1) and the land type are also indicated.

Site	Trap	Date	Cohort	T	Bank	Land	*N*	N C-T-Bank
Guiapet	4	10/2009	0	0	Left	Island	23	C0-T0-LeftBank
Yangoya	1	10/2009	0	0	Left	Island	30	53
Bakyia	1	05/2011	10	0	Left	Continent	11	
Bakyia	2	05/2011	10	0	Left	Continent	8	
Bakyia	3	05/2011	10	0	Left	Continent	5	
Guiapet	2	05/2011	10	0	Left	Island	7	
Guiapet	3	05/2011	10	0	Left	Island	4	C10-T0-LeftBank
Yangoya	1	05/2011	10	0	Left	Island	7	65
Yangoya	5	05/2011	10	0	Left	Island	3	
Yangoya	6	05/2011	10	0	Left	Island	2	
Yangoya	7	05/2011	10	0	Left	Island	16	
Yangoya	8	05/2011	10	0	Left	Island	2	
Dobire	6	05/2011	10	0	Right	Island	20	
Dobire	7	05/2011	10	0	Right	Island	12	C10-T0-RightBank
Santani	2	05/2011	10	0	Right	Continent	10	66
Santani	4	05/2011	10	0	Right	Continent	4	
Santani	5	05/2011	10	0	Right	Continent	20	
Bakyia	2	10/2019	61	92	Left	Continent	4	
Guiapet	2	10/2019	61	92	Left	Island	2	
Guiapet	3	10/2019	61	92	Left	Island	11	C61-TX-LeftBank
Yangoya	1	11/2019	61	93	Left	Island	2	35
Yangoya	5	11/2019	61	93	Left	Island	4	
Yangoya	6	11/2019	61	93	Left	Island	1	
Yangoya	7	11/2019	61	93	Left	Island	11	
Dobire	6	11/2019	67	33	Right	Island	9	
Dobire	7	10/2019	67	32	Right	Island	1	C61-TX-RightBank
Santani	2	11/2019	67	33	Right	Continent	8	27
Santani	4	11/2019	67	33	Right	Continent	1	
Santani	5	11/2019	67	33	Right	Continent	8	
Bakyia	2	10/2020	67	104	Left	Continent	3	
Guiapet	1	10/2020	67	104	Left	Island	15	C67-TX-LeftBank
Guiapet	2	10/2020	67	104	Left	Island	1	24
Yangoya	7	10/2020	67	104	Left	Island	5	
Dobire	1	10/2020	67	44	Right	Island	6	
Dobire	5	10/2020	67	44	Right	Island	2	C67-TX-RightBank
Santani	1	10/2020	67	44	Right	Continent	10	20
Santani	3	10/2020	67	44	Right	Continent	2	

N C-T-Bank: Names and numbers of riverbank subsamples, with the cohort (C) and the time (T) before (0) or after (X) the beginning of control.

Active surveillance began in 2011, where 2730 individuals (1474 females and 1256 males) were captured. In 2019, 143 flies (80 females and 63 males) and in 2020, 215 (106 females and 109 males) were caught. The details on number of flies in the different dates and locations, and all genotypes, are available in the supplementary file S1.

Assuming a two months generation time (Williams, 1990), as can be seen from Table 1, the genotyped subsamples extended from cohort 0 (2009), 10 (2011), 61 (2019) and 67 (2020). Because individuals belonging to one of these cohorts have no chance of interacting with any individual from another of these cohorts, we then always considered these four cohorts into separate entities.

Genotyping

Genotyping was undertaken for 11 loci: X55-3 (Solano et al., 1997), XpGp13, pGp24 (Luna et al., 2001), GPCAG (Baker & Krafsur, 2001), pGp15, pGp16, and pGp27 (Ravel et al., 2020). Loci A10, B3, XB104, C102 were kindly provided by A. Robinson (Insect Pest Control Sub-program, Joint Food and Agriculture Organization of the United Nations/International Atomic Energy Agency Program of Nuclear Techniques in Food and Agriculture). Despite used at several occasions (Camara et al., 2006; Bouyer et al., 2007; Solano et al., 2009; Melachio et al., 2011), information about these loci were never published. Readers will find this information in Table A1 in the Appendix. Locus name with an X means that the locus is located on the X chromosome, and thus haploid in males. Cells with a "0" correspond to individuals with no amplification at the concerned locus, while uninterpretable profiles were coded "NA" (see Supplementary file S1).

Data analyzed

Genotyping was undertaken in different ways and under different conditions for the different dates of sampling (see Table S1). For samples collected in 2009 and 2011, allele bands were resolved on a 4300 DNA Analysis System (LICOR, Lincoln, NE) using two infrared dyes (700 and 800nm) as described in (Solano et al., 2009). For samples collected in 2019 and 2020, an ABI 3500xl sequencer (Applied Biosystem, Waltham, Massachusetts) was used with four different dyes (FAM, NED, VIC and PET) as described in (Berté et al., 2019). Consequently, the 11 loci were not analyzed with the same dyes between samples from 2009-2011 and samples from 2019-2020. Because it is generally admitted that the dye used can modify the apparent size of the amplified alleles, we genotyped again some samples from 2009-2011 at the different loci using the ABI 3500xl sequencer to recode all the genotypes from the samples from 2009-2011 In some subsets,

too many missing data were observed at some loci or subsamples. Consequently, to avoid multiple analyses, keep a reasonable number of loci and for the sake of consistency, population genetics data analyses were undertaken with females only, at the eight loci that were successfully amplified over all the dataset (see Table S1): X55-3, XpGp13, pGp24, A10, B3, XB104, C102, and GPCAG.

Unless specified otherwise, the global dataset (File S1) was processed with Create (Coombs et al., 2008) to produce datasets in different formats, depending on the kind of analyses to be undertaken.

Selection of the relevant subsample units

The reproductive system of a population from a genotyped sample can be assessed through Wright's F_{IS} (Wright, 1965), which is a measure of the relative inbreeding of individuals as compared to the subpopulation they belong to. This parameter was estimated with Weir and Cockerham's unbiased estimator *f* (B. S. Weir & Cockerham, 1984), that we kept labelling F_{IS} for the sake of simplicity. In case of random mating in a dioecious population, a negative value is expected (Robertson, 1965; Pudovkin et al., 1996; Balloux, 2004; De Meeûs & Noûs, 2023). In tsetse flies, the trap can be the unit at which a significant subdivision may occur (Ravel et al., 2023), including *G. palpalis gambiensis* (Bouyer et al., 2009). Here, traps, and even sites, in combination with the cohort, often contained very few flies. To determine if traps, sites or river banks (right or left of the Pongo River, see Figure 1) really mattered, we used the Wahlund effect approach (Goudet et al., 1994; De Meeûs et al., 2006). We compared the F_{IS_T} in traps, the F_{IS_S} in sites (ignoring traps), the F_{IS_B} within the two riverbanks (ignoring sites), and the F_{IS_C} within the four cohorts (0, 10, 61 and 67) (ignoring river banks). For this, we undertook a Friedman two-way analysis of variance by ranks for data paired by locus with the package R-commander (J. Fox, 2005; J. Fox, 2007) (rcmdr) for R (R-Core-Team, 2022). We then undertook planned one sided Wilcoxon signed rank test for paired data. If traps and/or sites and/or river banks matter, we expect a Wahlund effect (De Meeûs et al., 2007; De Meeûs, 2018) when pooling individuals from different traps, and/or from different sites and or different river banks of the same cohort, meaning that the alternative hypothesis was $F_{IS_T} < F_{IS_S} < F_{IS_B} < F_{IS_C}$. When necessary (significant *p*-values), we corrected the *p*-values with the Benjamini and Yekutieli correction (Benjamini & Yekutieli, 2001) with R (command "p.adjust"), for test series with dependency.

178 *Quality testing of loci and subsamples*

179 Quality testing of the subsamples and genotyping was assessed with linkage
180 disequilibrium (LD), Wright's F_{IS} and F_{ST} (Wright, 1965) and their variance across loci.

181 Linkage disequilibrium was tested with the *G*-based randomization test between
182 each locus pair across subsamples as described in (De Meeûs et al., 2009), with 10,000
183 random shuffling of genotypes of the two loci of each pair. Because there are as many
184 non-independent tests as locus pairs, we adjusted the *p*-values with the Benjamini and
185 Yekutieli (BY) procedure with R (command "p.adjust").

186 Wright *F*-statistics were estimated with Weir and Cockerham's unbiased estimators
187 (B. S. Weir & Cockerham, 1984): f for F_{IS}, θ for F_{ST} and F for F_{IT}. Their significant deviation
188 from the expected value under the null hypothesis (H0: F_{IS}=0 or F_{ST}=0) was tested with
189 10,000 randomizations of alleles between individuals within subsamples (for F_{IS}) and of
190 individuals between subsamples (for F_{ST}). For F_{IS}, the statistic used was Weir and
191 Cockerham's f for each locus and overall. For testing subdivision we used the *G* based test
192 (Goudet et al., 1996) for each locus and overall. For F_{IS}, tests are one-sided (F_{IS}>0), and
193 two-sided *p*-values were obtained by doubling the one-sided *p*-value if <0.5 or we doubled
194 1-*p*-value otherwise. Confidence intervals (95%CI) were computed with 5000 bootstraps
195 over loci for the average over loci, and over individuals for the confidence intervals around
196 each locus. The standard error of jackknives over loci (SE) was computed for F_{IS} and F_{ST}
197 (SE_F_{IS} and SE_F_{ST} respectively) for null allele diagnostics (see below).

198 All this computations and randomizations were undertaken with Fstat 2.9.4 (Goudet,
199 2003), updated from Fstat 1.2 (Goudet, 1995), except the bootstraps over individuals, for
200 which we used Genetix (Belkhir et al., 2004). Since Genetix computes bootstraps for each
201 locus in each subsamples, we averaged these values across subsamples to obtain 95%CI
202 of F_{IS} for each locus.

203 Null allele signatures were looked for with several criterions: the ratio of SE of F_{IS}
204 over F_{ST} (r_{SE}), as computed with jackknives over loci; the correlation between F_{IS} and F_{ST},
205 and between F_{IS} and the number of missing genotypes (N_b) (De Meeûs, 2018). These
206 correlations were tested with a one-sided (positive correlation) Spearman's signed rank
207 correlation test. The regression F_{IS}~N_b was also undertaken to determine the proportion of
208 the variance of F_{IS} that was explained by missing genotypes (putative null homozygotes)
209 with the determination coefficient R^2, and to extrapolate the possible basic F_{IS} (F_{IS_0}) in
210 absence of null alleles through the intercept of this regression. Null allele frequencies were
211 also estimated with the EM algorithm (Dempster et al., 1977) implemented by FreeNA
212 (Chapuis & Estoup, 2007). For these analyses, missing genotypes (true blanks) were

213 coded as null homozygotes for allele 999, as recommended (Chapuis & Estoup, 2007).
214 The goodness of fit of observed blank genotypes, with the expected number of missing
215 data, was assessed with a one-sided exact binomial test with R (command "binom.test"). If
216 null alleles and random mating fully explain the data, there should be at least as many
217 blank genotypes as expected. For this test we computed the square of null allele
218 frequency of each locus in each subsample and multiplied it by the subsample size. To
219 increase statistical power, we summed these expected number of null homozygotes over
220 all subsamples ($N_{Exp\text{-}b}$) and compared those to the observed number of missing genotypes
221 for each locus, over all the considered dataset. We then also undertook the regression
222 F_{IS}~p_n, where p_n is the global null allele frequency.
223 Stuttering detection and correction followed the procedure described elsewhere (De
224 Meeûs et al., 2021; De Meeûs & Noûs, 2022) over all subsamples and for each locus,
225 using the associated template "TestStutterDioecious-n1000N100-1-10%Stuttering.xlsx"
226 available at https://zenodo.org/record/7029324, exact binomial tests and adjustment of *p*-
227 values with Benjamini and Hochberg (BH) procedure with R (command "p.adjust").
228 Short allele dominance (SAD) was looked for with the correlation method between
229 F_{IT} and the size of the alleles (Manangwa et al., 2019) using a one-sided (negative
230 relationship) Spearmans rank correlation test. In case of doubt, we also undertook the
231 regression F_{IS}~Allele size, weighted with $p_i(1\text{-}p_i)$, and where p_i was the frequency of the
232 allele (De Meeûs et al., 2004). Correlation and regression tests were undertaken with
233 rcmdr. For SAD, the regression allows to minimize spurious correlations due to rare
234 alleles. In rcmdr, regression tests are two-sided. To obtain a one-sided *p*-value, when the
235 slope was negative, we simply halved the two-sided *p*-value, or computed 1-*p*-value/2
236 otherwise. We labelled the correlation *p*-value p_{cor} and the regression one p_{reg}.
237
238 *Subdivision*
239 Comparisons of *F*-statistics between different subsamples or between F_{IS} and F_{IT}
240 was undertaken with Wilcoxon signed rank tests for paired data with rcmdr, using the loci
241 as pairing factor. Tests were one-sided in the appropriate direction (e.g. $F_{IT}>F_{IS}$).
242 Subdivision was measured and tested with Wright's F_{ST} and the *G* randomization test, as
243 described above. Genetic differentiation was measured tested between each pair of

244 cohorts in the same way, except that systematic paired test required BY corrections for
245 significant *p*-values.
246
247 *Effective population sizes and effective population densities*
248 We estimated effective population sizes (N_e) with several algorithms and softwares.
249 The first method is the heterozygote excess method from De Meeûs and Noûs (De Meeûs
250 & Noûs, 2023), computed for each locus in each cohort, ignoring values below or equal to
251 0, and averaged across loci, for each subsample (e.g. cohort). The second method was
252 the linkage disequilibrium based method (Waples & Do, 2010), corrected for missing data
253 (Peel et al., 2013), implemented by NeEstimator (Do et al., 2014), and assuming random
254 mating and selecting results for alleles with frequency above or equal to 5%. The third
255 method was the co-ancestry method (Nomura, 2008), also implemented by NeEstimator.
256 The fourth method used the averages obtained with four temporal methods. Three were
257 implemented in NeEstimator: Pollak, Nei and Tajima, and Jorde and Ryman (Nei & Tajima,
258 1981; Pollak, 1983; Jorde & Ryman, 2007) assuming random mating and selecting results
259 for alleles with frequency above or equal to 5%. For these three temporal method, we
260 averaged N_e across the different comparisons (different cohort pairs), ignoring "Infinite"
261 results The last temporal method was the maximum likelihood temporal method
262 implemented in MLNe (Wang & Whitlock, 2003). For MLNe, maximum and minimum
263 values corresponded to the confidence interval outputted by the procedure. We then
264 computed the average across all temporal methods, weighted by the number of usable
265 values and averaged minimum and maximum values in the same way. For MLNe, the
266 weight was the number of cohort pairs (6). The fifth method was the within and between
267 loci identity probabilities (Vitalis & Couvet, 2001b) with Estim (Vitalis & Couvet, 2001a).
268 The sixth method was the sibship frequency method (Wang, 2009) with Colony (Jones &
269 Wang, 2010), assuming female and male polygamy, and inbreeding. For each method, we
270 computed the average, the minimum and maximum across usable values, and assigned a
271 weight (number of usable values). For temporal methods, the weight was set to 4 (number
272 of cohorts). We then obtained the grand average for N_e and minimum and maximum
273 (minimax) values through an average across methods, weighted by the aforementioned
274 weights. This methodology obviously provided a rough approximation of N_e and the space
275 of its possible values, and finding the most accurate way will need specific multi-scenarios
276 simulation approaches, as discussed elsewhere (De Meeûs & Noûs, 2023).
277 To compute effective population densities, we considered three different surfaces,
278 computed with the function "insert a polygon" of Google Earth Pro. The smallest area was

defined by the traps containing flies that were indeed genotyped, as in Figure 1 and Table 1, and labelled S_{Genet}=132 km². The second surface was defined by all traps that captured at least one tsetse fly in 2011, during the most extensive survey campaign (Kagbadouno et al., 2012) (see File S1), S_C=224 km². The third area was defined by the limits of the survey defined before 2011 (see File S1); S_L=629 km². The largest surface was drawn considering all "mangrove-like" environments in Google Earth Pro, S_{max}=1301 km². Effective population densities were then computed by dividing the effective population size by these surfaces. For the sake of comparison, we also computed the densities of captured flies in 2011 (initial survey, T0), in 20019 and 2020 (see Files S1 for raw data). We also compute the sex-ratios of captured (c) flies, $SR=N_{c\text{-males}}/N_{c\text{-females}}$ with these data. The homogeneity of the proportion of females across cohorts was tested with a Fisher exact test with rcmdr. The evenness of sex-ratios was then tested with a two-sided exact binomial test with R (command "binom.test").

Finally, maximum distances between the most remote sites defined by each aforementioned surface was computed with Google Earth Pro with the menu "Add a trajectory".

Bottleneck signatures

We tried to find bottleneck signatures with the diversity excess method and the Wilcoxon signed rank test method with Bottleneck (Cornuet & Luikart, 1996), with a particular interest to subsamples genotyped after the beginning of control (cohorts 61 and 67). We used the three mutation models: IAM, TPM with default options, and SMM. Significant signatures of a bottleneck can be suspected if the test is highly significant with the IAM and significant with the TPM at least. Weaker signals tend to be produced in population with very small effective population sizes (TdM, unpublished simulation results).

Results

Defining the relevant geographic scales for subsample units

There was no significant difference between F_{IS_T}, F_{IS_S} and F_{IS_B} (all p-values>0.4) (Figure 2). We thus ignored traps, sites and river banks for further analyses, and kept only the different cohorts (cohorts 0, 10, 61 and 67) as subsample units.

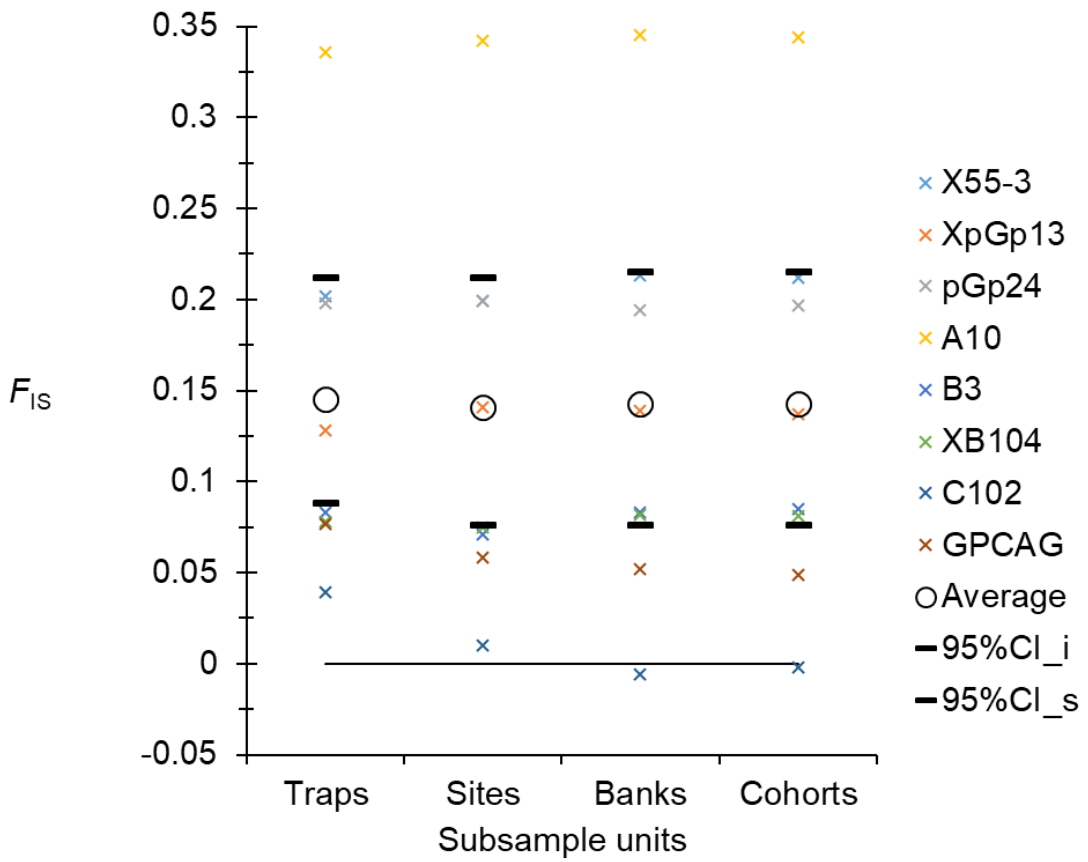

Figure 2: Comparisons of F_{IS} within traps (F_{IS_T}), within sites (ignoring traps) (F_{IS_S}), within river banks (ignoring sites) (F_{IS_B}), and within each cohort (ignoring river banks) (F_{IS_C}) in female subsamples of *Glossina palpalis gambiensis* across 11 years in the mangroves of Boffa, Guinea, for eight loci (crosses of different colors), average (empty circles) and 95%CI (black dashes). The global comparison outputted a *p*-value=0.9663 and none of paired tests provided a *p*-value<0.4.

Quality testing of the subsamples and loci

Only one locus pair out of 28 appeared in significant LD (less than 4%) (*p*-value=0.039). It did not remain significant after BY correction. We thus considered all loci to be statistically independent from each other's.

There was a substantial but variable heterozygote deficit: F_{IS}= 0.143 in 95%CI=[0.076, 0.215] (*p*-value<0.0002) (Figure 3). With r_{SE}=19, and the positive correlation between F_{IS} and F_{ST} (ρ=0.5988, *p*-value=0.0584), we could suspect that most of this heterozygote deficit could be explained by null alleles. Nevertheless, the correlation between F_{IS} and N_b did not seem to confirm this (ρ=0.0952, *p*-value=0.4201). Nonetheless, this lack of signal resulted from three outlier loci (pGp24, B3 and C102), which displayed too many missing genotypes as regard to their relatively low F_{IS} (Figure 3). This means that many of these missing data, at these three loci, probably did not correspond to true null homozygotes.

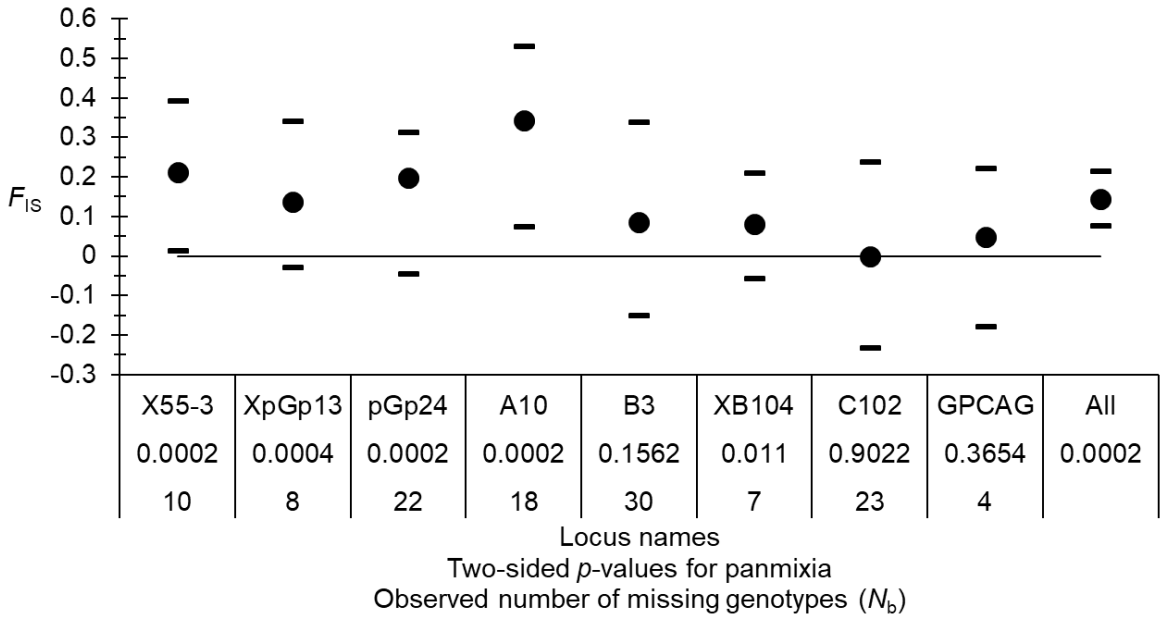

Figure 3: Variation of F_{IS} across loci in the four cohorts of *Glossina palpalis gambiensis* from Boffa (Guinea). Averages (black dots), and 95% confidence intervals (black dashes) were computed by 5000 bootstraps over individuals (for each locus) and over loci (All). The two sided *p*-values for significant deviation from panmixia and the number of observed missing genotypes are also provided.

We thus undertook the correlation and the regression F_{IS}~N_b without these three loci. The results can be observed in the Figure 4. The correlation became significant and the regression suggested that missing genotypes (null alleles) explains almost all (96%) of F_{IS} variation. The intercept was negative, as expected in small, pangamic dioecious populations (F_{IS_0}=-0.0412 in 95%CI=[-0.1872, 0.1171]).

For null allele frequency estimates, we recoded as homozygous for the null allele (allele coded 999) all missing genotypes but for the three outlier loci. Indeed, for these loci, most missing data (coded "0", and kept as such) probably corresponded to another problem. With these data, estimate of null allele frequencies, and the resulting expected number of missing data over all subsamples fitted very well with the observed ones at each locus (all *p*-values>0.2). Moreover, the regression F_{IS}~p_n displayed very good results (R^2=0.8566, F_{IS_0}=0.012 in 95%CI=[-0.1951, 0.2143]).

We also undertook the stuttering and SAD analyses. We found a significant stuttering signature for locus A10 only (*p*-value=0.0286). Nevertheless, null alleles explained this locus well enough (Figures 3 and 4) so that we could consider this result as coincidental. Three loci displayed marginally significant signatures of SAD: X55-3 (p_{cor}=0.0423, p_{reg}=0.1551), pGp24 (p_{cor}=0.0963, p_{reg}=0.0489), and B3 (p_{cor}=0.288, p_{reg}=0.4841). Given the weakness of such results, and that these three loci are very well

358 explained by null alleles, we did not consider that any locus was affected by SAD, and that
359 a few null alleles randomly associated with small alleles provided these weak signatures.
360 We detected no Wahlund effect and the significant heterozygote deficits observed
361 were entirely caused by null alleles of frequencies 0.02 to 0.28.
362

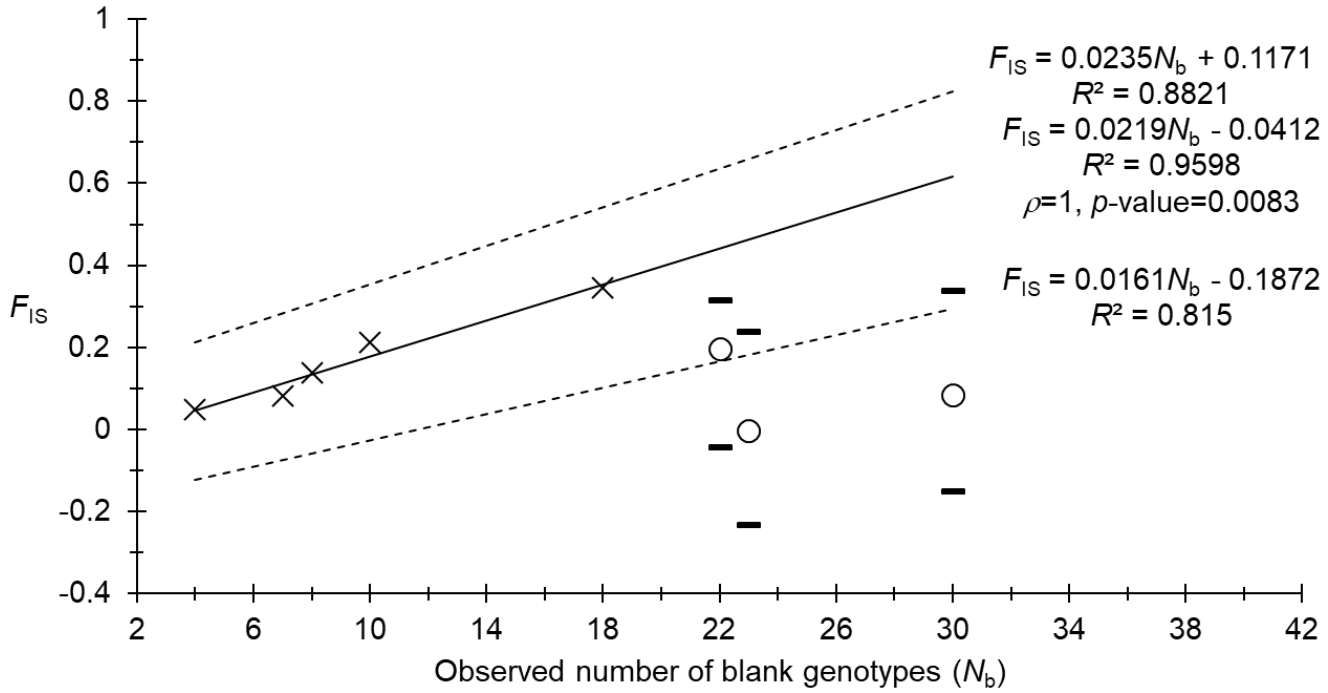

363
364 Figure 4: Regression of F_{IS} by the number of missing genotypes (black crosses and
365 continuous line) without loci displaying an excess of missing genotypes (pGp24, B3 and
366 C102) (empty circles) and of the corresponding 95%CI of bootstraps over individuals for
367 *Glossina palpalis gambiensis* from Boffa (Guinea) (black dashes and broken lines).
368 Regression equations, the determination coefficient (R^2) and the result of the correlation
369 test are also given.
370
371 Average subdivision was globally not significant with a weak variance across the
372 different loci: F_{ST}=-0.001 in 95%CI=[-0.004, 0.004] (p-value=0.6938). In particular, GPCAG
373 displayed a negative value: F_{ST}=-0.007 (-0.006 with FreeNA correction) (p-value=0.1709),
374 and allele 219 (here labelled 220, due to probable lag produced by the change in size
375 calibration on this species), did not increase in frequency after control had begun: 0.094,
376 0.093, 0.065, and 0.022 for cohorts 0, 10, 61 and 67, respectively.
377
378 *Subdivision*
379 As demonstrated above, we could not detect any geographic subdivision signature.
380 Subdivision was globally weak across the different cohorts: average F_{ST}=-0.001 in
381 95%CI=[-0.004, 0.004] and not significant (p-value=0.6938). Moreover, F_{IT}=0.142 in

95%CI=[0.073, 0.218] was not significantly bigger than F_{IS}=0.143 in 95%CI=[0.076, 0.215] (*p*-value=0.7695).

We also measured and tested subdivision between each pair of cohorts. In the Figure 5, we can confirm the absence of any subdivision. Moreover, subdivision between cohorts before control (T0) and after control had begun (TX) did not appear bigger than for other cohort comparisons.

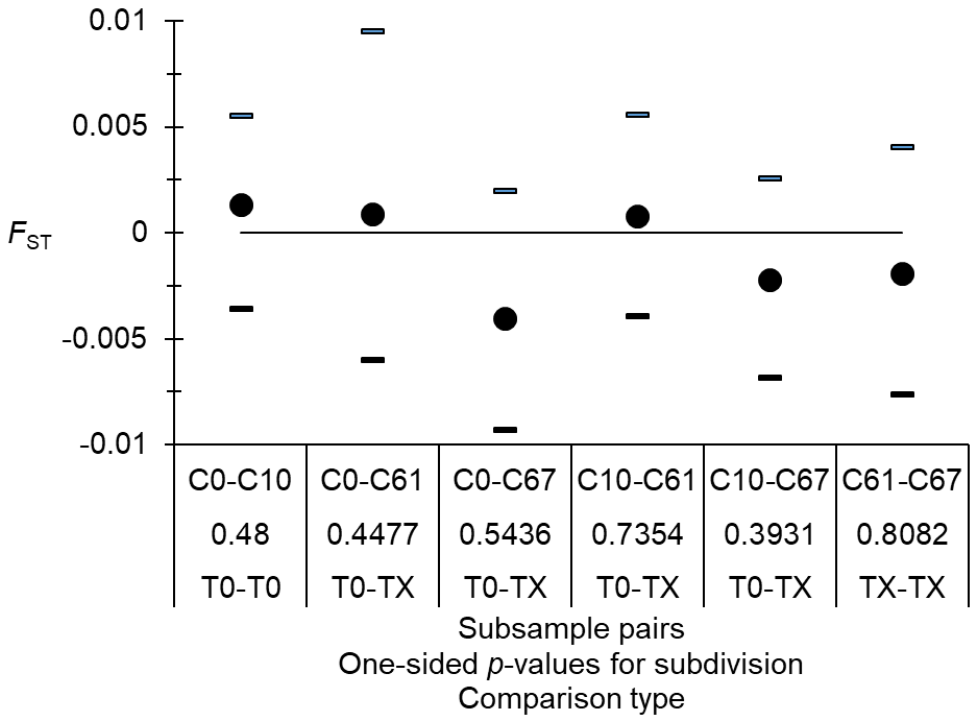

Figure 5: Subdivision measures (F_{ST}) and test between each pair of cohorts (C0, C10, C61 and C67). The result of the test (*p*-values) and the comparison type between cohorts before control (T0) or after the beginning of control (TX) are also indicated.

Effective population sizes and effective population densities

For this section, Estim provided no usable values. For the remaining methods, results are presented in the Table 2. These values were quite variable, but did not display particularly smaller values after control (26 and 18 for cohorts 61 and 67 respectively) than before control (22 and 42 for cohorts 0 and 10 respectively). Nevertheless, such comparisons could only be made for the heterozygote excess, co-ancestries and sibships methods.

Table 2: Effective population size, minimum and maximum values estimated with different methods, and over all method (average weighted with "Weight"). Codes for methods are HzEs: heterozygote excess; LD: linkage disequilibrium; CoAn: coancestries.

	Methods					
	HzEs	LD	CoAn	Temporal	Sibship	Over all
Average	14	461	24	15130	44.5	3830
Minimum	5	461	21	404	32	143
Maximum	24	461	28	18957	73	4798
Weight	4	1	3	4	4	

Taking the surface occupied by genotyped flies, the resulting effective population density was $D_{e\text{-Genet}}$=8 in minimax=[1, 17] flies per km². However, given the absence of any population subdivision signature, we considered that this quantity was a very strong overestimate. In the Figure 6, we can see the effective population densities computed with S_C, S_L and S_{max}.

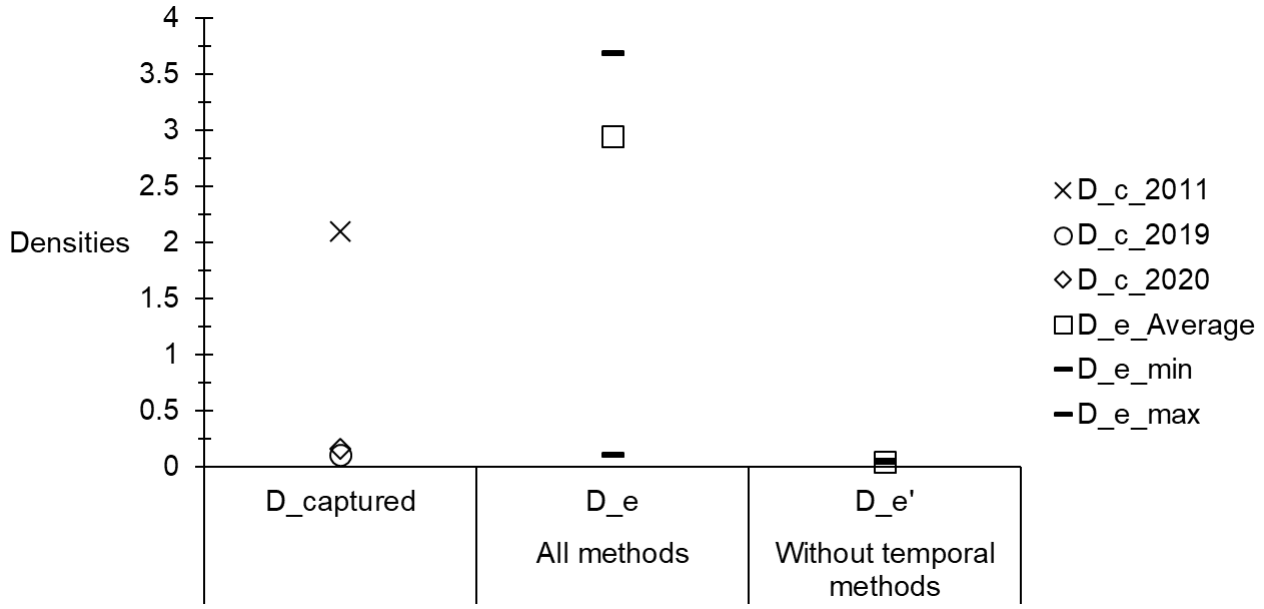

Figure 6: Densities of captured flies (Dc) and corresponding effective population densities (De) while considering the whole surface of Boffa (as defined in the text) occupied by tsetse flies in the HAT focus of Boffa (Guinea), for different years and different effective population size averages: with all methods, or without temporal methods.

There was no significant variations of the sex ratio across years (0.85, 0.79 and 1.03 for 2011, 2019 and 2020 respectively) (*p*-value=0.3253). Combining all years, captured flies displayed a highly significant female biased sex ratio *SR*=0.86 (*p*-value<0.0001).

Capturing flies after control had begun, in the same trapping sites, obviously appeared more difficult than before control (Figure 6).

The maximum distances between the most remote points were 19 km, 40 km, 44 km and 62 km for the areas S_{Genet}, S_C, S_L and S_{max} respectively. Depending on the true area occupied by the population of tsetse flies in Boffa, these may represent the average dispersal distances from one generation to the next.

Bottleneck signatures

The results of these analyses are given in Table 3, where an absence of any bottleneck signature can be noticed, in particular after the beginning of control (cohorts 61 and 67).

Table 3: One sided *p*-values for the detection of a genetic signature of a bottleneck with the three models of mutation (IAM, TPM and SMM) for the different subsamples before the beginning of vector control (Cohorts 0 and 10) and after the beginning of control (Cohorts 61 and 67).

Cohort	IAM	TPM	SMM
Cohort 0	0.3711	0.9629	0.9981
Cohort 10	0.6289	0.9980	1
Cohort 61	0.5781	0.9863	0.9961
Cohort 67	0.6289	0.6797	1

Discussion

Despite the presence of null alleles, the eight loci studied here in female *G. palpalis gambiensis* converged with the existence of a large pangamic population of this species occupying the HAT focus of Boffa. This was confirmed by the absence of any Wahlund effect when pooling all individuals from all the sampling area into one subsample in each cohort. The regression of the F_{IS} with null alleles or number of missing data, with a determination coefficient close to unity and a negative intercept confirmed this perception. Subdivision tests also confirmed a free migration of tsetse flies in the area defined by this tsetse population. Taking the total surface where flies could be captured and the total surface of the survey, as the most realistic values, the corresponding dispersal distance would be between 40 and 44 km per generation. The constant shading, high humidity and wind conditions of the particular continuously favorable mangrove ecosystem probably explain such important values (Courtin et al., 2010; Courtin & Kagbadouno, 2011; Courtin et al., 2015). Within these surfaces, the effective population density could be considered to vary between 3 and 6 individuals per km², in minimax≈[0.1, 8]. These range within the smallest values as compared to what can be found elsewhere (De Meeûs et al., 2019).

457 This is even worse if we consider that, here, we could use temporal methods for estimating
458 effective population sizes. Temporal methods are almost never available in the literature,
459 but provided very high values in the present study. Without temporal methods, densities
460 would have fallen to very small values: between 0.05 and 0.1 individuals per km² only, for
461 the two surfaces respectively.
462 We observed a significant female biased *SR* in this population with small effective
463 population densities. In a recent study of *G. fuscipes fuscipes* from Chad (Ravel et al.,
464 2023), authors found a negative correlation between *SR* and densities. Scattered
465 distribution of hosts, leading to smaller effective population densities of the flies, would
466 impose to these insects to travel more to find blood meals. Because of larval feeding,
467 female tsetse would need to feed more often than males and be captured more often than
468 those in such kind of ecological frameworks. On the contrary, abundance of hosts would
469 maintain dense populations of tsetse flies, with no need to spend time seeking for blood
470 meals, especially so for females, while males still need looking for mates.
471 The absence of any significant genetic differentiation between subsamples before
472 and after the beginning of control, especially at locus GPCAG, of any strong (if any) effect
473 on effective population sizes, and the total absence of any genetic signature of a
474 bottleneck, testify of an absence of consequences of the VCC on the genetic structure of
475 this tsetse population, at the scale of the focus. Nevertheless, the dramatic drop in
476 captured flies after the VCC had begun, indicated an efficient protection of the human
477 population against tsetse bites around the targeted zones. The drop in tsetse bites and
478 HAT prevalence and incidence in selected controlled zones has already proved such a
479 protection (Courtin et al., 2015). It also indicates that in the areas targeted by vector
480 control tsetse densities would probably regain initial levels rapidly in case of scaling back.
481 The fact that a significant decrease in HAT prevalence was observed
482 (https://apps.who.int/neglected_diseases/ntddata/hat/hat.html) also advocates for the
483 benefic effects of the VCC. Finally, the absence of impact on the targeted population at the
484 scale of the whole mangrove of Boffa, suggests that VCC as it was undertaken, is efficient
485 at protecting human populations, but does not significantly affect the biodiversity of this
486 particular ecosystem.
487 In conclusion, due to the difficulties to access to all tsetse-infested zones, where
488 multiple hosts are available for these blood feeding insects, maintaining control measures
489 in zones frequented by human populations seems a reasonable measure, in order to
490 protect these populations from tsetse bites and subsequent transmission of HAT. Given
491 that the existence of hidden human and/or animal reservoirs can be suspected, such a

492 measure appears mandatory for now and a close future, before more research results
493 shed more light on the eco-epidemiology of this deadly disease in mangrove ecosystems.
494
495 **Acknowledgements**
496
497
498 **Funding**
499 This work was funded by the Bill & Melinda Gates Foundation
500 (http://www.gatesfoundation.org, grant agreement INV-001785)" and the JEAI RECIT
501 (#400982/00) of the IRD.
502
503 **Conflict of interest disclosure**
504 The authors declare that they comply with the PCI rule of having no financial
505 conflicts of interest in relation to the content of the article
506
507 **Author contributions**
508 Moise S. Kagbadouno: data collection, data analyses and manuscript correction.
509 Modou Séré: genotyping, data analyses and manuscript correction.
510 Adeline Ségard: genotyping and manuscript correction.
511 Abdoulaye Dansy Camara: data collection and manuscript correction.
512 Mamadou Camara: supervision and manuscript correction.
513 Bruno Bucheton: supervision, data collection and manuscript correction.
514 Jean-Mathieu Bart: supervision, data collection and manuscript correction.
515 Fabrice Courtin: supervision, data collection and manuscript correction.
516 Thierry de Meeûs: supervision, data analyses, writing of the manuscript and design of
517 figures.
518 Sophie Ravel: supervision, genotyping and manuscript correction.
519
520 **Data, scripts, code, and supplementary information availability**
521 Raw data are available at https://zenodo.org/record/8181166. For data analyses, all
522 R scripts used are inserted in the main text. For other analyses we used facilities without
523 the need of scripts (e.g. click and point programs or packages).
524

References

Baker MD, Krafsur ES (2001) Identification and properties of microsatellite markers in tsetse flies *Glossina morsitans* sensu lato (Diptera: Glossinidae). *Molecular Ecology Notes,* **1**, 234-236. https://doi.org/https://doi.org/10.1046/j.1471-8278.2001.00087.x

Balloux F (2004) Heterozygote excess in small populations and the heterozygote-excess effective population size. *Evolution,* **58**, 1891-1900. https://doi.org/https://doi.org/10.1554/03-692

Belkhir K, Borsa P, Chikhi L, Raufaste N, Bonhomme F (2004) GENETIX 4.05, logiciel sous Windows TM pour la génétique des populations. Laboratoire Génome, Populations, Interactions, CNRS UMR 5000, Université de Montpellier II, Montpellier (France). https://doi.org/https://kimura.univ-montp2.fr/genetix/

Benjamini Y, Yekutieli D (2001) The control of the false discovery rate in multiple testing under dependency. *The Annals of Statistics,* **29**, 1165–1188. https://doi.org/ https://doi.org/10.1214/aos/1013699998

Berté D, De Meeus T, Kaba D, Séré M, Djohan V, Courtin F, N'Djetchi KM, Koffi M, Jamonneau V, Ta BTD, Solano P, N'Goran EK, Ravel S (2019) Population genetics of *Glossina palpalis palpalis* in sleeping sickness foci of Côte d'Ivoire before and after vector control. *Infection Genetics and Evolution,* **75**, 103963. https://doi.org/https://doi.org/10.1016/j.meegid.2019.103963

Bouyer J, Balenghien T, Ravel S, Vial L, Sidibé I, Thévenon S, Solano P, De Meeûs T (2009) Population sizes and dispersal pattern of tsetse flies: rolling on the river? *Molecular Ecology,* **18**, 2787-2797. https://doi.org/ https://doi.org/10.1111/j.1365-294X.2009.04233.x

Bouyer J, Dicko AH, Cecchi G, Ravel S, Guerrini L, Solano P, Vreysen MJB, De Meeûs T, Lancelot R (2015) Mapping landscape friction to locate isolated tsetse populations candidate for elimination. *Proceedings of the National Academy of Sciences of the*

551 *United States of America,* **112**, 14575–14580.
552 https://doi.org/https://doi.org/10.1073/pnas.1516778112
553 Bouyer J, Ravel S, Dujardin JP, De Meeûs T, Vial L, Thévenon S, Guerrini L, Sidibe I,
554 Solano P (2007) Population structuring of *Glossina palpalis gambiensis* (Diptera:
555 Glossinidae) according to landscape fragmentation in the Mouhoun river, Burkina
556 Faso. *Journal of Medical Entomology,* **44**, 788-795.
557 https://doi.org/https://doi.org/10.1603/0022-2585(2007)44[788:psogpg]2.0.co;2
558 Bucheton B, Kheir MM, El-Safi SH, Hammad A, Mergani A, Mary C, Abel L, Dessein A
559 (2002) The interplay between environmental and host factors during an outbreak of
560 visceral leishmaniasis in eastern Sudan. *Microbes and Infection,* **4**, 1449-1457.
561 https://doi.org/https://doi.org/10.1016/s1286-4579(02)00027-8
562 Büscher P, Bart JM, Boelaert M, Bucheton B, Cecchi G, Chitnis N, Courtin D, Figueiredo
563 LM, Franco JR, Grébaut P, Hasker E, Ilboudo H, Jamonneau V, Koffi M, Lejon V,
564 MacLeod A, Masumu J, Matovu E, Mattioli R, Noyes H, Picado A, Rock KS,
565 Rotureau B, Simo G, Thévenon S, Trindade S, Truc P, Van Reet N (2018) Do
566 cryptic reservoirs threaten gambiense-sleeping sickness elimination? *Trends in*
567 *Parasitology,* **34**, 197-207. https://doi.org/10.1016/j.pt.2017.11.008
568 Camara M, Caro-Riano H, Ravel S, Dujardin JP, Hervouet JP, De Meeûs T, Kagbadouno
569 MS, Bouyer J, Solano P (2006) Genetic and morphometric evidence for population
570 isolation of *Glossina palpalis gambiensis* (Diptera : Glossinidae) on the Loos
571 islands, Guinea. *Journal of Medical Entomology,* **43**, 853-860.
572 https://doi.org/https://doi.org/10.1603/0022-2585(2006)43[853:gamefp]2.0.co;2
573 Chapuis MP, Estoup A (2007) Microsatellite null alleles and estimation of population
574 differentiation. *Molecular Biology and Evolution,* **24**, 621-631.
575 https://doi.org/10.1093/molbev/msl191

576 Coombs JA, Letcher BH, Nislow KH (2008) CREATE: a software to create input files from
577 diploid genotypic data for 52 genetic software programs. *Molecular Ecology*
578 *Resources,* **8**, 578–580. https://doi.org/https://doi.org/10.1111/j.1471-
579 8286.2007.02036.x
580 Cornuet JM, Luikart G (1996) Description and power analysis of two tests for detecting
581 recent population bottlenecks from allele frequency data. *Genetics,* **144**, 2001-2014.
582 https://doi.org/https://doi.org/10.1093/genetics/144.4.2001
583 Courtin F, Camara M, Rayaisse JB, Kagbadouno M, Dama E, Camara O, Traore IS,
584 Rouamba J, Peylhard M, Somda MB, Leno M, Lehane MJ, Torr SJ, Solano P,
585 Jamonneau V, Bucheton B (2015) Reducing human-tsetse contact significantly
586 enhances the efficacy of sleeping sickness active screening campaigns: a
587 promising result in the context of elimination. *PLoS Neglected Tropical Diseases,* **9**.
588 https://doi.org/10.1371/journal.pntd.0003727
589 Courtin F, Jamonneau V, Camara M, Camara O, Coulibaly B, Diarra A, Solano P,
590 Bucheton B (2010) A geographical approach to identify sleeping sickness risk
591 factors in a mangrove ecosystem. *Tropical Medicine & International Health,* **15**,
592 881-889. https://doi.org/10.1111/j.1365-3156.2010.02559.x
593 Courtin F, Kagbadouno M (2011) Peuplements, mobilités et paysages en zone de
594 mangrove guinéenne : le cas de la baie de Sangaréah (Guinée). *Les Cahiers*
595 *d'Outre-Mer,* **256**, 453-466. https://doi.org/10.4000/com.6358
596 De Meeûs T (2018) Revisiting F_{IS}, F_{ST}, Wahlund effects, and Null alleles. *Journal of*
597 *Heredity,* **109**, 446-456. https://doi.org/10.1093/jhered/esx106
598 De Meeûs T, Chan CT, Ludwig JM, Tsao JI, Patel J, Bhagatwala J, Beati L (2021)
599 Deceptive combined effects of short allele dominance and stuttering: an example
600 with *Ixodes scapularis*, the main vector of Lyme disease in the U.S.A. *Peer*
601 *Community Journal,* **1**, e40. https://doi.org/https://doi.org/10.24072/pcjournal.34

602 De Meeûs T, Guégan JF, Teriokhin AT (2009) MultiTest V.1.2, a program to binomially
603 combine independent tests and performance comparison with other related
604 methods on proportional data. *BMC Bioinformatics,* **10**, 443.
605 https://doi.org/https://doi.org/10.1186/1471-2105-10-443
606 De Meeûs T, Humair PF, Grunau C, Delaye C, Renaud F (2004) Non-Mendelian
607 transmission of alleles at microsatellite loci: an example in *Ixodes ricinus*, the vector
608 of Lyme disease. *International Journal for Parasitology,* **34**, 943-950.
609 https://doi.org/https://doi.org/10.1016/j.ijpara.2004.04.006
610 De Meeûs T, Lehmann La, Balloux F (2006) Molecular epidemiology of clonal diploids: A
611 quick overview and a short DIY (do it yourself) notice. *Infection Genetics and*
612 *Evolution,* **6**, 163-170. https://doi.org/https://doi.org/10.1016/j.meegid.2005.02.004
613 De Meeûs T, McCoy KD, Prugnolle F, Chevillon C, Durand P, Hurtrez-Boussès S, Renaud
614 F (2007) Population genetics and molecular epidemiology or how to "débusquer la
615 bête". *Infection Genetics and Evolution,* **7**, 308-332.
616 https://doi.org/https://doi.org/10.1016/j.meegid.2006.07.003
617 De Meeûs T, Noûs C (2022) A simple procedure to detect, test for the presence of
618 stuttering, and cure stuttered data with spreadsheet programs. *Peer Community*
619 *Journal,* **2**, e52. https://doi.org/https://doi.org/10.24072/pcjournal.165
620 De Meeûs T, Noûs C (2023) A new and almost perfectly accurate approximation of the
621 eigenvalue effective population size of a dioecious population: comparisons with
622 other estimates and detailed proofs *Peer Community Journal,* **3**, e51.
623 https://doi.org/https://doi.org/10.24072/pcjournal.280
624 De Meeûs T, Ravel S, Solano P, Bouyer J (2019) Negative density dependent dispersal in
625 tsetse flies: a risk for control campaigns? *Trends in Parasitology,* **35**, 615-621.
626 https://doi.org/https://doi.org/10.1016/j.pt.2019.05.007

Dempster AP, Laird NM, Rubin DB (1977) Maximum likelihood from incomplete data via the EM algorithm. *Journal of the Royal Statistical Society Series B,* **39**, 1–38. https://doi.org/http://links.jstor.org/sici?sici=0035-9246%281977%2939%3A1%3C1%3AMLFIDV%3E2.0.CO%3B2-Z

Do C, Waples RS, Peel D, Macbeth GM, Tillett BJ, Ovenden JR (2014) NeEstimator v2: re-implementation of software for the estimation of contemporary effective population size (N_e) from genetic data. *Molecular Ecology Resources,* **14**, 209-214. https://doi.org/https://doi.org/10.1111/1755-0998.12157

Fox J (2005) The R commander: a basic statistics graphical user interface to R. *Journal of Statistical Software,* **14**, 1–42. https://doi.org/https://doi.org/10.18637/jss.v014.i09

Fox J (2007) Extending the R commander by "plug in" packages. *R News,* **7**, 46–52. https://doi.org/https://stat.ethz.ch/pipermail/r-help/attachments/20071101/3603125e/attachment.pdf

Goudet J (1995) FSTAT (Version 1.2): A computer program to calculate F-statistics. *Journal of Heredity,* **86**, 485-486. https://doi.org/https://doi.org/10.1093/oxfordjournals.jhered.a111627

Goudet J (2003) Fstat (ver. 2.9.4), a program to estimate and test population genetics parameters. Available at http://www.t-de-meeus.fr/Programs/Fstat294.zip, Updated from Goudet (1995).

Goudet J, De Meeûs T, Day AJ, Gliddon CJ (1994) The different levels of population structuring of dogwhelks, *Nucella lapillus*, along the south Devon coast. In: *Genetics and Evolution of Aquatic Organisms* (ed. Beaumont A), pp. 81-95. Chapman and Hall, London.

Goudet J, Raymond M, De Meeûs T, Rousset F (1996) Testing differentiation in diploid populations. *Genetics,* **144**, 1933-1940. https://doi.org/https://doi.org/10.1093/genetics/144.4.1933

653 Holmes P (2014) First WHO meeting of stakeholders on elimination of gambiense human
654 african trypanosomiasis. *PLoS Neglected Tropical Diseases,* **8**, e3244.
655 https://doi.org/https://doi.org/10.1371/journal.pntd.0003244
656 Jamonneau V, Truc P, Grébaut P, Herder S, Ravel S, Solano P, De Meeus T (2019)
657 *Trypanosoma brucei gambiense* group 2: the unusual suspect. *Trends in*
658 *Parasitology,* **35**, 983-995. https://doi.org/https://doi.org/10.1016/j.pt.2019.09.002
659 Jones OR, Wang JL (2010) COLONY: a program for parentage and sibship inference from
660 multilocus genotype data. *Molecular Ecology Resources,* **10**, 551-555.
661 https://doi.org/10.1111/j.1755-0998.2009.02787.x
662 Jorde PE, Ryman N (2007) Unbiased estimator for genetic drift and effective population
663 size. *Genetics,* **177**, 927-935.
664 https://doi.org/https://doi.org/10.1534/genetics.107.075481
665 Kagbadouno MS, Camara M, Rouamba J, Rayaisse JB, Traoré IS, Camara O,
666 Onikoyamou MF, Courtin F, Ravel S, De Meeûs T, Bucheton B, Jamonneau V,
667 Solano P (2012) Epidemiology of sleeping sickness in boffa (Guinea): where are the
668 trypanosomes? *PLoS Neglected Tropical Diseases,* **6**, e1949.
669 https://doi.org/10.1371/journal.pntd.0001949
670 Koffi M, De Meeûs T, Bucheton B, Solano P, Camara M, Kaba D, Cuny G, Ayala FJ,
671 Jamonneau V (2009) Population genetics of *Trypanosoma brucei gambiense*, the
672 agent of sleeping sickness in Western Africa. *Proceedings of the National Academy*
673 *of Sciences of the United States of America,* **106**, 209-214.
674 https://doi.org/https://doi.org/10.1073/pnas.0811080106
675 Koffi M, De Meeûs T, Séré M, Bucheton B, Simo G, Njiokou F, Salim B, Kaboré J,
676 MacLeod A, Camara M, Solano P, Belem AMG, Jamonneau V (2015) Population
677 genetics and reproductive strategies of african trypanosomes : revisiting available

678 published data. *PLoS Neglected Tropical Diseases,* **9**, e0003985.
679 https://doi.org/https://doi.org/10.1371/journal.pntd.0003985
680 Luna C, Bonizzoni MB, Cheng Q, Aksoy S, Zheng L (2001) Microsatellite polymorphism in
681 the tsetse fies (Diptera: Glossinidae). *Journal of Medical Entomology,* **38**, 376–381
682 Manangwa O, De Meeûs T, Grébaut P, Segard A, Byamungu M, Ravel S (2019) Detecting
683 Wahlund effects together with amplification problems : cryptic species, null alleles
684 and short allele dominance in Glossina pallidipes populations from Tanzania.
685 *Molecular Ecology Resources,* **19**, 757-772.
686 https://doi.org/https://doi.org/10.1111/1755-0998.12989
687 Melachio T, T. T., Simo G, Ravel S, De Meeûs T, Causse S, Solano P, Lutumba P,
688 Asonganyi T, Njiokou F (2011) Population genetics of Glossina palpalis palpalis
689 from central African sleeping sickness foci. *Parasites and Vectors,* **4**, 140.
690 https://doi.org/10.1186/1756-3305-4-140
691 Nei M, Tajima F (1981) Genetic drift and estimation of effective population size. *Genetics,*
692 **98**, 625-640. https://doi.org/https://doi.org/10.1093/genetics/98.3.625
693 Nomura T (2008) Estimation of effective number of breeders from molecular coancestry of
694 single cohort sample. *Evolutionary Applications,* **1**, 462-474.
695 https://doi.org/https://doi.org/10.1111%2Fj.1752-4571.2008.00015.x
696 Peel D, Waples RS, Macbeth GM, Do C, Ovenden JR (2013) Accounting for missing data
697 in the estimation of contemporary genetic effective population size (N_e). *Molecular*
698 *Ecology Resources,* **13**, 243-253. https://doi.org/https://doi.org/10.1111/1755-
699 0998.12049
700 Pollak E (1983) A new method for estimating the effective population size from allele
701 frequency changes. *Genetics,* **104**, 531-548.
702 https://doi.org/https://doi.org/10.1093/genetics/104.3.531

703 Pudovkin AI, Zaykin DV, Hedgecock D (1996) On the potential for estimating the effective
704 number of breeders from heterozygote excess in progeny. *Genetics,* **144**, 383-387.
705 https://doi.org/https://doi.org/10.1093/genetics/144.1.383
706 R-Core-Team (2022) R: A Language and Environment for Statistical Computing (Version
707 4.2.2 (2022-10-31 ucrt)).
708 Ravel S, Mahamat MH, Ségard A, Argiles-Herrero R, Bouyer J, Rayaisse J-B, Solano P,
709 Mollo BG, Pèka M, Darnas J, Belem AMG, Yoni W, Noûs C, De Meeûs T (2023)
710 Population genetics of *Glossina fuscipes fuscipes* from southern Chad. *Peer*
711 *Community Journal,* **3**, e31. https://doi.org/https://doi.org/10.24072/pcjournal.257
712 Ravel S, Sere M, Manangwa O, Kagbadouno M, Mahamat MH, Shereni W, Okeyo WA,
713 Argiles-Herrero R, De Meeûs T (2020) Developing and quality testing of
714 microsatellite loci for four species of *Glossina*. *Infection Genetics and Evolution,* **85**,
715 104515. https://doi.org/https://doi.org/10.1016/j.meegid.2020.104515
716 Robertson A (1965) The interpretation of genotypic ratios in domestic animal populations.
717 *Animal Production,* **7**, 319-324.
718 https://doi.org/https://doi.org/10.1017/S0003356100025770
719 Ségard A, Romero A, Ravel S, Truc P, Dobigny G, Gauthier P, Etougbetche J, Dossou H-
720 J, Badou S, Houéménou G, Morand S, Chaisiri K, Noûs C, De Meeûs T (2022)
721 Development of nine microsatellite loci for *Trypanosoma lewisi*, a potential human
722 pathogen in Western Africa and South-East Asia, and preliminary population
723 genetics analyses. *Peer Community Journal,* **2**, e69.
724 https://doi.org/https://doi.org/10.24072/pcjournal.188
725 Simarro PP, Cecchi G, Franco JR, Paone M, Diarra A, Priotto G, Mattioli RC, Jannin JG
726 (2015) Monitoring the Progress towards the Elimination of Gambiense Human
727 African Trypanosomiasis. *PLoS Neglected Tropical Diseases,* **9**, e0003785.
728 https://doi.org/10.1371/journal.pntd.0003785

729 Solano P, Duvallet G, Dumas V, Cuisance D, Cuny G (1997) Microsatellite markers for
730 genetic population studies in *Glossina palpalis* (Diptera: Glossinidae). *Acta Tropica,*
731 **65**, 175-180
732 Solano P, Ravel S, Bouyer J, Camara M, Kagbadouno MS, Dyer N, Gardes L, Herault D,
733 Donnelly MJ, De Meeûs T (2009) The population structure of *Glossina palpalis*
734 *gambiensis* from island and continental locations in coastal Guinea. *PLoS*
735 *Neglected Tropical Diseases,* **3**, e392. https://doi.org/10.1371/journal.pntd.0000392
736 Vitalis R, Couvet D (2001a) ESTIM 1.0: a computer program to infer population
737 parameters from one- and two-locus gene identity probabilities. *Molecular Ecology*
738 *Notes,* **1**, 354-356. https://doi.org/https://doi.org/10.1046/j.1471-8278.2001.00086.x
739 Vitalis R, Couvet D (2001b) Estimation of effective population size and migration rate from
740 one- and two-locus identity measures. *Genetics,* **157**, 911-925.
741 https://doi.org/https://doi.org/10.1093/genetics/157.2.911
742 Wang JL (2009) A new method for estimating effective population sizes from a single
743 sample of multilocus genotypes. *Molecular Ecology,* **18**, 2148-2164.
744 https://doi.org/https://doi.org/10.1111/j.1365-294X.2009.04175.x
745 Wang JL, Whitlock MC (2003) Estimating effective population size and migration rates
746 from genetic samples over space and time. *Genetics,* **163**, 429-446.
747 https://doi.org/https://doi.org/10.1093/genetics/163.1.429
748 Waples RS, Do C (2010) Linkage disequilibrium estimates of contemporary N_e using
749 highly variable genetic markers: a largely untapped resource for applied
750 conservation and evolution. *Evolutionary Applications,* **3**, 244-262.
751 https://doi.org/https://doi.org/10.1111/j.1752-4571.2009.00104.x
752 Weir BS, Cockerham CC (1984) Estimating F-statistics for the analysis of population
753 structure. *Evolution,* **38**, 1358-1370. https://doi.org/https://doi.org/10.1111/j.1558-
754 5646.1984.tb05657.x

755 Weir W, Capewell P, Foth B, Clucas C, Pountain A, Steketee P, Veitch N, Koffi M, De
756 Meeûs T, Kaboré J, Camara M, Cooper A, Tait A, Jamonneau V, Bucheton B,
757 Berriman M, MacLeod A (2016) Population genomics reveals the origin and asexual
758 evolution of human infective trypanosomes. *eLife,* **5**, e11473.
759 https://doi.org/https://doi.org/10.7554%2FeLife.11473
760 Williams BG (1990) Tsetse fly (Diptera: Glossinidae) population dynamics and the
761 estimation of mortality rates from life-table data. *Bulletin of Entomological Research,*
762 **80**, 479-485. https://doi.org/http://dx.doi.org/10.1017/S0007485300050756
763 Wright S (1965) The interpretation of population structure by F-statistics with special
764 regard to system of mating. *Evolution,* **19**, 395-420.
765 https://doi.org/https://doi.org/10.1111/j.1558-5646.1965.tb01731.x
766
767

768 **Appendix**

769

770 Appendix 1: Information on unpublished microsatellite loci

771

772 Table A1: Information on microsatellite loci provided by A. Robinson (Insect Pest Control
773 Sub-program, Joint Food and Agriculture Organization of the United Nations/International
774 Atomic Energy Agency Program of Nuclear Techniques in Food and Agriculture) used in
775 the present study. Name of primers motif, annealing temperature (T_ann in °C), the range
776 of sizes of amplified fragments, and primers' sequences are indicated.

Locus	Primers (5'-3')		Motif	T_ann	Size range
A10			(CA)	54.5	190
	A10F	GCAACGCCAAGTGAAATAAAG			
	A10R	TACTGGGCTCGCGTACATAAT			
B3			(GA)	55	181-195
	B3F	TTCGCTTTTGTCAGAAGTG			
	B3R	TCCCAGACGGTTCATATTAC			
XB104			(GA)	52	171-227
	B104F	ACGATTGTTCTTCTTCATTCC			
	B104R	AAGAAGCCAAACTTTCAACGCTCGC			
C102			(TGA)	52	257-278
	C102F	CGTTAAATTGTCACGATGAAG			
	C102R	AGCACATTTTTGGTACATTTATACC			

777

778 Touch-down PCR reactions were the same as in (Ségard et al., 2022):

N
W
E
S
Santani traps 1, 5
Santani traps 2, 4
Bakyia trap 3
Bakyia traps 1, 2
Guiapet trap 1
Guiapet traps 2, 3, 4
Dobire traps 6, 7
Rio Pongo
Yangoya traps 1, 5, 6, 7
0 4 8 km